DOI:10.33667/2782-4101-2022-2-17-21

RESULTS of MORPHOLOGICAL ANALYSIS of ANIMAL HARD TISSUES IN NORMAL AND SIMULATED OSTEOPOROSIS USING A NON–INVASIVE COMPUTED MICROTOMOGRAPHY TECHNIQUE

Alexander Dolgalev[1], Igor Rzhepakovsky[2], Aslan Danaev[1], Vazgen Avanisyan[1], Galina Shulga[1], Artemy Korobkeev[1]

[1]Stavropol State Medical University of the Ministry of Health of the Russian Federation, Stavropol, Russian Federation
[2]North-Caucasus Federal University of the Ministry of Science and Higher Education of the Russian Federation, Stavropol, Russian Federation

SUMMARY

Introduction. *X-ray microtomography is a non-destructive method of microstructural analysis, which has a high level of detail and allows the possibility of assessing the internal architecture of organs and tissues using 3D-analysis[1]. The specifics of working with such equipment can be divided into in vivo and in vitro, i.e. working with live laboratory animals (mice, rats, rabbits) under anesthesia or studying organs and tissues separated from the animal [2].*

The aim of the work *was to study the microstructure of sheep bone tissues in normal and simulated osteoporosis using computed microtomography.*

Materials and methods. *We performed microCT analysis of different sheep bones in normal and experimental osteoporosis. Bone tissue of the jaw, iliac and femur, and teeth were collected from control and experimental animals. Bone tissue samples were fixed in 10% buffered formalin. X-ray microCT scanner Skyscan 1176 (Bruker-microCT, Belgium) and software Skyscan 1176 control program (10.0.0.0), Nrecon (1.7.4.2), DataViewer (1.5.6.2), CT-analyser (1.18.4.0), CTvox (3.3.0r1403) were used to scan and process materials.*

Results. *MicroCT examination and 3D-imaging confirmed the elimination of trabeculae in the metaphyseal region of the femur in sheep with experimental osteoporosis from the centre to the periphery; in addition, 3D-analysis showed a 15.1% decrease in bone percentage, a 7.8% decrease in bone mineral density, and an increase in Tb. Sp. (trabecular separation), Tb. Pf. (trabecular pattern factor) and SMI (structure model index) by 30.2%, 20.8% and 23.6%, respectively, and a decrease in Tb.N. (trabecular number) index by 18.6%, indicating calcium washout, decreased trabecular connectivity and a transition from a lamellar to a rod-like architecture. Similar changes were found in the 3D-analysis of the jaw bone tissue. Thus, a decrease of 18.9% in mineral density was found, as well as a significant increase of 11.58 and 2.21 in the indices, particularly Tb. Pf. and SMI. 3D-analysis of iliac microtomography also indicates a simulation of osteoporosis, as evidenced by a significant increase in the main indices characterising the development of this pathology.*

Conclusions. *The obtained results not only objectively testify to the development of osteoporosis in the experimental animals, but also indicate signs of the adaptation-compensatory reactions of the body, characterized by appearance of large single trabeculae in the metaphysis of the femur as well as by not expressed reduction of bone mineral density and bone tissue area.*

KEYWORDS: *microtomography; nondestructive testing; imaging; bone tissue; osteoporosis; medicine.*

CONFLICT of INTEREST. *The authors declare no conflicts of interest.*

Introduction

Osteoporosis is a progressive metabolic disease of the skeleton, in which there is a generalised reduction of bone mass and bone structure that differs from the age and sex norm, leading to a decrease in physical bone strength and the risk of fractures even with minor trauma. Bone strength is determined by a combination of quantitative and qualitative characteristics: bone mineral density and architectonics, bone metabolism, damage accumulation, and tissue mineralisation. Computed microtomography provides accurate quantitative data on these characteristics without compromising the integrity of the samples under study. [3]

Microtomography is one of the main methods of non-destructive analysis and one of the most common methods of microscopy [1], which visualises the very fine internal structure of objects to provide high-resolution volumetric data at the micron level. This enables the study of microstructures, the precise determination of geometry [4–7], eventually defects and differences in density and morphology. It does not require sample preparation, staining and slicing; settings and parameters have been extensively studied for specific structures [8]. It has great potential for biomedical and bioengineering applications [9]. MicroCT systems are present as laboratory instruments in major laboratories and companies for various types of research and applications including educational purposes [10,11]. Analyses carried out using microtomography can also be useful in terms

of compliance with international standards, regulations and in forensic practice [12, 13]. Microtomography analyses can influence the material validation process and quality assessment of finished devices.

Dentistry and Oral and Maxillofacial Surgery (O&M) represent two sectors that influence the biomedical engineering context and where microtomography is widely used because of the need for detailed information on small and complex objects, mineralised structures and with varying densities. The market is characterised by innovative materials and solutions requiring advanced technology in the routine activities of dental laboratories and clinics, such as microtomography [14,15], whose capabilities prove indispensable.

The aim of the work was to study the microstructure of sheep bone tissue in normal and simulated osteoporosis using computed microtomography.

Materials and methods

Bone tissue samples fixed in 10% buffered formalin in accordance with the rules for pathomorphological and histological studies were the objects of study [2].

The samples presented:

Sample № 1

Bone tissue of sheep's jaw in the normal state.

Sample № 2

Bone tissue of sheep's jaw in osteoporosis simulation

Sample № 3

Sheep's tooth in the normal state.

Sample № 4

Osteoporosis simulation in a sheep's tooth

Sample № 5

Sheep femur in the normal state

Sample № 6

Sheep femur in osteoporosis modeling

Sample № 7

Sheep ileum in the normal state

Sample № 8

Sheep ileum in osteoporosis simulation

To study the structure of sheep bones and determine their bone mineral density (BMD), a Skyscan 1176 (Bruker) X-ray computer microCT scanner was used [16]. The system allows creating 3D-reconstructions of objects with resolution up to 9 microns, making it possible to study the structure and density of the examined object without damaging its integrity.

Each bone was scanned along with two phantoms (0.25 and 0.75 g/cm3 calcium hydroxyapatite Ca5(PO4)3(OH)) with the diameter corresponding to the thickness of the examined samples.

Scanning parameters in the Skyscan 1176 control program (10.0.0.0, Bruker-microCT, Belgium):

Sample № 1

X-ray voltage 80 kV, X-ray current 300 µA, filter Cu+Al, image pixel size 8,87 µm, tomographic rotation 180°, rotation step 0,3, frame averaging 4.

Sample № 2

X-ray voltage 65 kV, X-ray current 380 µA, filter 0,5 mm Al, image pixel size 8,87 µm, tomographic rotation 180°, rotation step 0,3, frame averaging 4.

Sample № 3

X-ray voltage 90 kV, X-ray current 270 µA, filter Cu 0,1 mm, image pixel size 8,87 µm, tomographic rotation 180°, rotation step 0,3, frame averaging 3.

Sample № 4

X-ray voltage 90 kV, X-ray current 270 µA, filter Cu 0,1 mm, image pixel size 8,87 µm, tomographic rotation 180°, rotation step 0,3, frame averaging 3.

Sample № 5

X-ray voltage 90 kV, X-ray current 259 µA, filter Cu 0,1 mm, image pixel size 35,47 µm, tomographic rotation 180°, rotation step 0,6, frame averaging 4.

Sample № 6

X-ray voltage 90 kV, X-ray current 259 µA, filter Cu 0,1 mm, image pixel size 35,47 µm, tomographic rotation 180°, rotation step 0,6, frame averaging 4.

Sample № 7

X-ray voltage 80 kV, X-ray current 291 µA, filter filter Cu+Al, image pixel size 35,47 µm, tomographic rotation 180°, rotation step 0,3, frame averaging 4.

Sample № 8

X-ray voltage 80 kV, X-ray current 291 µA, filter filter Cu+Al, image pixel size 35,47 µm, tomographic rotation 180°, rotation step 0,3, frame averaging 4.

The scanned objects were reconstructed in Nrecon (1.7.4.2, Bruker-microCT, Belgium) with the following basic reconstruction parameters:

Sample № 1

smoothing 2, ring reduction 10, beam hardening 41, minimum for CS to Image Conversion=0,002, maximum for CS to Image Conversion=0,04.

Sample № 2

smoothing 2, ring reduction 10, beam hardening 41, minimum for CS to Image Conversion=0.002, maximum for CS to Image Conversion=0,08.

Sample № 3

smoothing 4, ring reduction 20, beam hardening 41, minimum for CS to Image Conversion=0.002, maximum for CS to Image Conversion=0,038.

Sample № 4

smoothing 4, ring reduction 20, beam hardening 41, minimum for CS to Image Conversion=0.002, maximum for CS to Image Conversion=0,038.

Sample № 5

smoothing 2, ring reduction 20, beam hardening 41, minimum for CS to Image Conversion=0,002, maximum for CS to Image Conversion=0,03.

Sample № 6

smoothing 2, ring reduction 20, beam hardening 41, minimum for CS to Image Conversion=0,002, maximum for CS to Image Conversion=0,03.

Sample № 7

smoothing 2, ring reduction 20, beam hardening 41, minimum for CS to Image Conversion=0,000, maximum for CS to Image Conversion=0,03.

Sample № 8

smoothing 2, ring reduction 20, beam hardening 41, minimum for CS to Image Conversion=0,000, maximum for CS to Image Conversion=0,03.

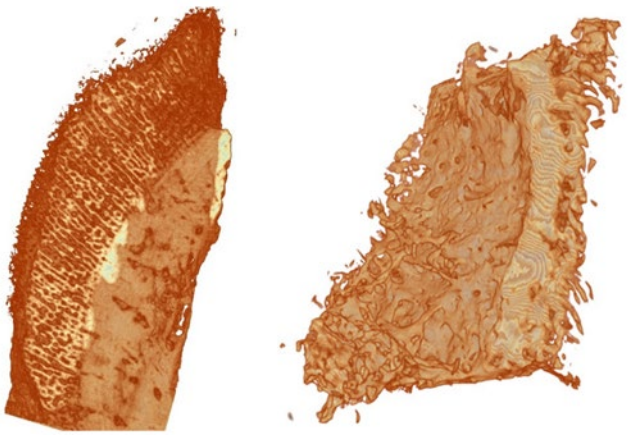

Sample № 1. The bone tissue of a sheep's jaw in normal state.

Sample № 2. The bone tissue of the sheep's jaw in osteoporosis simulation.

Fig.1. Comparison of samples № 1 and № 2.

Table 1

Results of microtomography analysis of sheep jaw bones in osteoporosis simulation

Name of samples	BMD, g/cm³ (bone tissue in trabeculae only)	Tb.Pf (1/mm) *	SMI **
Sample № 1	0,815	-2,35	-0,46
Sample № 2	0,661	9,23	1,75
The difference	**-18,9%**	**на 11,58**	**на 2,21**

*Note: *Trabecular pattern factor, **Structure model index.*

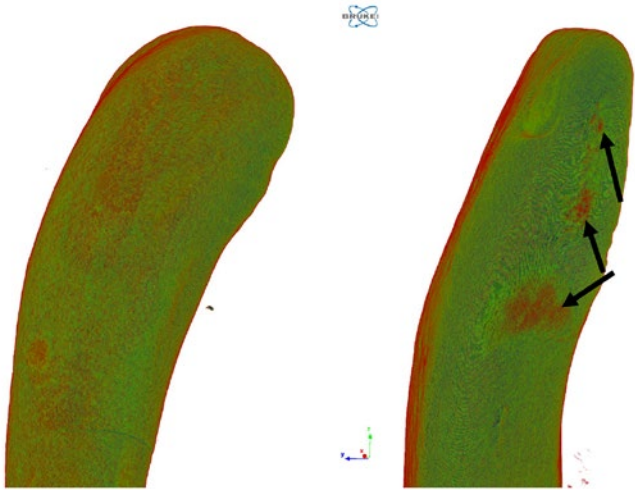

Sample № 3. Sheep's tooth in the normal state

Sample № 4. A sheep's tooth in an osteoporosis simulation. Arrows mark areas of enamel erosion. X-ray density increases from red to green.

Fig. 2. Comparison of samples № 3 and № 4.

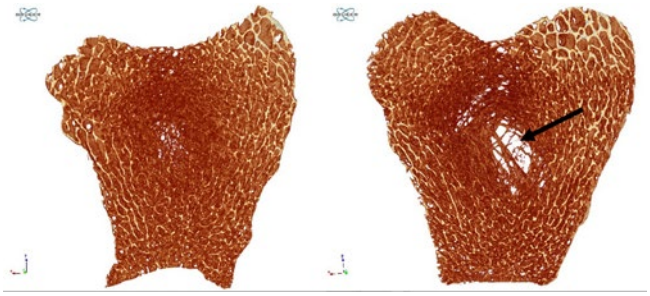

Sample № 5. Trabecular structure in the metaphyseal area of the sheep femur in the normal state.

Sample № 6. Trabecular structure in the metaphyseal region of the sheep femur in the osteoporosis simulation. An arrow marks the area of trabecular elimination, and the formation of few thickened trabeculae is also detected.

Fig. 3. Comparison of samples № 5 and № 6.

Orientation (x, y, z) and isolation of individual regions of reconstructed materials was performed in DataViewer (1.5.6.2, Bruker-microCT, Belgium).

Visualization, data analysis and BMD determination were performed in the CT-analyser software (1.18.4.0, Bruker-microCT, Belgium). According to the manufacturer's official guidelines, the software was first calibrated using phantoms, followed by the BMD determination in the different VOI samples. A 3D-visualisation of the results obtained as a function of radiological density was performed in the CTvox software (3.3.0r1403, Bruker-microCT, Belgium).

Results

Examination of samples by microtomography and 3D-analysis showed a decrease of trabecular tissue mineral density in Sample № 2 by 0.154 g/cm3 (18.9%) (*Fig. 1*), a significant increase of indices, in particular Tb. Pf. and SMI by 11.58 and 2.21 indicating calcium wash-out and thinning of trabeculae, reduction of trabecular connectivity and their transition from plate-like to rod-like architecture (*Tab. 1*). This type of change is characteristic of osteoporosis.

Numerous enamel erosions are visualised in the microCT analysis of the teeth of a sheep in which osteoporosis has been simulated (*Fig. 2*).

The state of osteoporosis was also confirmed by the main method, microtomography of the femur bones of sheep (*Fig. 3*). a 3D-analysis of the metaphysis of the femur of an animal with simulated osteoporosis showed a 15.1% decrease in bone percentage, a 7.8% decrease in bone mineral density as well as an increase in indices, particularly Tb. Sp., Tb. Pf. and SMI by 30.2%, 20.8% and 23.6% respectively and a decrease in Tb.N. index by 18.6% (*Tab. 2*). This indicates

Table 2

Results of microtomography analysis of sheep femurs in osteoporosis simulation

Name of samples	BV/TV,%	BMD, r/см³	Tb.Th, mm	Tb.N, (1/mm) *	Tb.Sp, mm **	Tb.Pf (1/mm) ***	SMI ****
Sample № 5	23,2	0,284	0,271	0,86	2,25	1,44	0,72
Sample № 6	19,7	0,262	0,283	0,7	2,93	1,74	0,89
The difference	**-15,1%**	**-7,8%**	**+4,4%**	**-18,6%**	**+30,2%**	**+20,8%**	**+23,6%**

*Note: *Trabecular number, **Trabecular separation ***Trabecular pattern factor (Tb. Pf), ****Structure model index (SMI).*

Sample № 7. Trabecular structure of the sheep's iliac bone in normal state.

Sample № 8. Trabecular structure of sheep ileum in osteoporosis simulation.

Fig. 4. Comparison of samples № 7 and № 8.

calcium washout and thinning of the trabeculae, decreased connectivity between the trabeculae, and a change from a lamellar to a rod-like architecture, which is characteristic of osteoporosis.

Moreover, additional 3D-analysis of iliac microtomography (*Fig. 4*), also indicates the development of osteoporosis, which is confirmed by a significant increase of 80.6 % and 81.5 % in the main indices characterising this pathology, Tb. Pf. and SMI, respectively (*Tab. 3*).

Findings

Examination of samples by microtomography and 3D-analysis showed a decrease of mineral density of trabecular tissue in sample № 2 by 0,154 g/cm3 (18,9 %), significant increase of indices, in particular Tb. Pf. and SMI by 11,58 and 2,21 indicating calcium washout and thinning of trabeculae, reduction of the connection level between trabeculae and their change from plate-like to rod-like architecture which is typical for osteoporosis.

Numerous enamel erosions are visualized in the microCT analysis of the teeth of a sheep in which osteoporosis has been simulated.

The condition of osteoporosis was confirmed by the main method, microCT of the femoral bones of sheep. a 3D-analysis of the metaphysis of the femur of the animal with simulated osteoporosis showed a 15.1 % decrease in bone percentage, a 7.8 % decrease in bone mineral density and an increase in the indices, particularly Tb. Sp, Tb. Pf. and SMI by 30.2 %, 20.8 % and 23.6 %, respectively, and a decrease in Tb. N. index by 18.6 %, indicating calcium washout and thinning of the trabeculae, a reduction in the level of communication between the trabeculae and their transition from a lamellar to a rod-like architecture, which is characteristic of osteoporosis.

Moreover, additional 3D-analysis of iliac microtomography also indicates a pattern of osteoporosis, which is confirmed by a significant increase of 80.6 % and 81.5 % in the main indices characterizing the development of this pathology, Tb. Pf. and SMI, respectively.

Conclusions

The obtained results objectively indicate the development of osteoporosis in experimental animals, but also indicate signs of adaptation-compensatory reactions of the body. These reactions are characterized by the appearance of large trabeculae in the metaphyseal area of the femur, an unexpressed decrease in bone mineral density and bone tissue area, especially in the iliac bone. Such morphological analysis would not have been possible without the use of computed tomography techniques. The conventional methods of histological examination with slices, macro- and microspecimens are not able to quantify the magnitude of osteoporosis and assess the degree of bone deformation. When examining the hard tissues in experimental animals, it is reasonable to use methods of examination without damaging the integrity of the examined samples, because it will be impossible to visualise and reconstruct the qualitative and quantitative indicators of conducted work. It is the objectivity and clarity of this technique that enables us to recommend its use for the evaluation of bone tissue in various experimental studies, so necessary for clinicians of various specialisations.

References

1. *Grande, N.M.; Plotino, G.; Gambarini, G.; Testarelli, L.; D'Ambrosio, F.; Pecci, R.; Bedini, R. Present and future in the use of microCT scanner 3D-analysis for the study of dental and root canal morphology. Ann. Ist. Super. Sanità 2012, 48, 26–34.*
2. *Korzhevsky D.E., Gilyarov A.V. Fundamentals of histological technique.– SPb.: SpetsLit, 2010.– 95 p.*
3. *Charwat-Pessler, J.; Musso, M.; Petutschnigg, A.; Entacher, K.; Plank, B.; Wernersson, E.; Tangl, S.; Schuller-Gotzburg, P. a bone sample containing a bone graft substitute analyzed by correlating density information obtained by X-ray micro tomography with compositional information obtained by raman microscopy. Materials 2015, 8, 3831–3853.*
4. *Daly, S.M. Biophotonics for Blood Analysis; Elsevier: Amsterdam, The Netherlands, 2015; ISBN9780857096746.*
5. *Campioni, I.; Cacciotti, I.; Gupta, N. Additive manufacturing of reconstruction devices for maxillofacial surgery: Design and accuracy assessment of a mandibular plate prototype. Ann. Ist. Super. Sanità 2020, 56, 10–18.*
6. *Mangione, F.; Meleo, D.; Talocco, M.; Pecci, R.; Pacifici, L.; Bedini, R. Comparative evaluation of the accuracy of linear measurements between cone beam computed tomography and 3D-microtomography. Ann. Ist. Super. Sanità 2013, 49, 261–265.*
7. *Sinibaldi, R.; Pecci, R.; Somma, F.; Penna, S.D.; Bedini, R. a new software for dimensional measurements in 3D-endodontic root canal instrumentation. Ann. Ist. Super. Sanità 2012, 48, 42–48.*
8. *Vögtlin, C.; Schulz, G.; Jäger, K.; Müller, B. Comparing the accuracy of master models based on digital intraoral scanners with conventional plaster casts. Phys. Med. 2016, 1, 20–26.*

Table 3

Results of microtomography analysis of sheep iliac bones in osteoporosis simulation

Name of sampes	BV/TV,%	BMD, r/см^3	Tb.Th, mm	Tb.N, (1/mm) *	Tb.Sp, mm **	Tb.Pf (1/mm) ***	SMI****
Sample № 7	26,7	0,331	0,188	1,42	0,71	0,72	0,27
Sample № 8	26,4	0,318	0,192	1,38	0,65	1,3	0,49
The difference	**-1,1 %**	**+3,9 %**	**+2,1 %**	**-2,8 %**	**-8,5 %**	**+80,6 %**	**+81,5 %**

*Note: *Trabecular number, **Trabecular separation, ***Trabecular pattern factor (Tb. Pf), ****Structure model index (SMI).*

9. Cengiz, I.F.; Oliveira, J.M.; Reis, R.L. Micro-computed tomography characterization of tissue engineering scaffolds: Effects of pixel size and rotation step. J. Mater. Sci. Mater. Med. 2017, 28.
10. Boerckel, J.D.; Mason, D.E.; McDermott, A.M.; Alsberg, E. Microcomputed tomography: Approaches and applications in bioengineering. Stem Cell Res. Ther. 2014, 5, 1–12
11. Liao, C.-W.; Fuh, L.-J.; Shen, Y.-W.; Huang, H.-L.; Kuo, C.-W.; Tsai, M.-T.; Hsu, J.-T. Self-assembled micro-computed tomography for dental education. PLoS ONE2018, 13, e0209698.
12. Deyhle, H.; Schmidli, F.; Krastl, G.; Müller, B. Evaluating tooth restorations: Micro-computed tomography in practical training for students in dentistry. Int. Soc. Optical Eng. 2010, 7804, 780417.
13. Sandholzer, M.A.; Walmsley, A.D.; Lumley, P.J.; Landini, G. Radiologic evaluation of heat-induced shrinkage and shape preservation of human teeth using microCT. J. Forensic Radiol. Imaging 2013, 1, 107–111.
14. Rutty, G.N.; Brough, A.; Biggs, M.J.P.; Robinson, C.; Lawes, S.D.A.; Hainsworth, S.V. The role of micro-computed tomography in forensic investigations. Forensic Sci. Int. 2013, 225, 60–66.
15. Leeson, D. The digital factory in both the modern dental lab and clinic. Dent. Mater. 2019, 1, 43–52.
16. Bouxsein M.L., Boyd S.K., Christiansen B.A., Guldberg R.E., Jepsen K.J., Muller R. Guidelines for assessment of bone microstructure in rodents using micro–computed tomography // Journal of Bone and Mineral Research. 2010. Vol. 25, N7. P. 1468–1486. DOI:10.1002/jbmr.141.

Received 15.07.2022
Revised 18.07.2022
Accepted 23.07.2022

INFORMATION ABOUT AUTHORS

Dolgalev Alexander Alexandrovich, *PhD, MD, Head of the Center for Innovation and Technology Transfer, Professor of the Department of General Practice Dentistry and Pediatric Dentistry of Stavropol State Medical University of the Ministry of Health of the Russian Federation, Professor of the Department of Clinical Dentistry with a course of OS and MFS of Pyatigorsk Medical and Pharmaceutical Institute-branch of the Volgograd State Medical University, Stavropol, Russian Federation. ORCID: https://orcid.org/0000-0002-6352-6750. Tel. +79624404861, e-mail: dolgalev@dolgalev.pro*

Rzhepakovsky Igor Vladimirovich, *Candidate of Biological Sciences, Associate Professor at the Department of Applied Biotechnology, leading researcher of the interdepartmental research and education laboratory of experimental immunomorphology, immunopathology and immunobiotechnology, North-Caucasus Federal University, Stavropol, Russian Federation. Tel. +79054164981, e-mail: irzhepakovskii@ncfu.ru*

Danaev Aslan Baradinovich, *Head of the Saverclinica Centre for Training in the Basics of Lean Manufacturing in Health Care at the institute of additional professional education, Stavropol State Medical University of the Ministry of Health of the Russian Federation, Stavropol, Russian Federation. ORCID: https://orcid.org/0000-0003-4754-3101. Tel. +79289111148, e-mail: aslandanaev111@mail.ru*

Avanisyan Vazgen Mikhailovich, *the 5-th grade student of the Faculty of Dentistry of the Stavropol State Medical University of the Ministry of Health of the Russian Federation, Stavropol, Russian Federation. ORCID: https://orcid.org/0000-0002-0316-5957. Tel. +79286338995, e-mail: avanvaz@yandex.ru*

Shulga Galina Sergeevna, *the 4-th grade student of the Faculty of Dentistry of the Stavropol State Medical University of the Ministry of Health of the Russian Federation, Stavropol, Russian Federation. ORCID: https://orcid.org/0000-0003-2328-6948. Tel. +79288266451 e-mail: g.dolgopolowa2015@yandex.ru*

Korobkeev Artemy Aleksandrovich, *the 3-th grade student of the Faculty of Dentistry of the Stavropol State Medical University of the Ministry of Health of the Russian Federation, Stavropol, Russian Federation. ORCID: https://orcid.org/0000-0001-6188-2578. Tel. +79624429874, e-mail: korobkeevartemy@gmail.com*

DOI:10.33667/2782-4101-2022-2-21-26

TISSUE–ENGINEERED BONE IMPLANTS FOR THE REPLACEMENT OF JAWBONE DEFECTS. LITERATURE REVIEW

Konstantin Kobets, Artak Kazaryan, Saddam Bopkhoev

Peoples' Friendship University of Russia (RUDN University), 6 Miklukho-Maklaya St., Moscow, 117198, Russian Federation

SUMMARY

The purpose of the study: *to trace the development of methods of bone implants for the replacement of jawbone defects: from ceramic and polymeric scaffolds to complex tissue-engineered structures with stem cells, growth factors and vascular anastomoses based on literature data.*

Materials and methods: *searching, systematization and analysis of scientific data on various types of 3D-printed bone implants and their effectiveness in replacing bone defects.*

Conclusions: *Modern technologies of 3D-printing, cell and tissue engineering, microvascular surgical techniques closely approach scientists and clinicians to creation of an artificial bone implant which in the body must become a living structure capable of integrating with the patient's bone. Only complex approach which includes reconstruction of the implant of individual shape and sufficient mechanical strength, giving of osteoinductive and osteogenic properties, providing of internal axial and external angiogenesis is the basis for such tissue-engineered construction.*

KEYWORDS: *artificial tissue implants, bone vascularisation, bone implants, bone engineering, bone the defects reconstruction, arteriovenous loop.*

CONFLICT of INTEREST. *The authors declare no conflict of interest.*